

Predominant (6,5) Single-Walled Carbon Nanotube Growth on a Copper-Promoted Iron Catalyst

Maoshuai He,^{*,†} Alexander I. Chernov,[‡] Pavel V. Fedotov,[‡] Elena D. Obratsova,[‡] Jani Sainio,[§] Emma Rikkinen,[†] Hua Jiang,^{||} Zhen Zhu,^{||} Ying Tian,^{||} Esko I. Kauppinen,^{*,||,⊥} Marita Niemelä,[†] and A. Outi I. Krause[†]

Department of Biotechnology and Chemical Technology, School of Science and Technology, Aalto University, P.O. Box 16100, FI-00076 Aalto, Finland, A. M. Prokhorov General Physics Institute, Russian Academy of Sciences, 38 Vavilov Street, 119991 Moscow, Russia, Department of Applied Physics, School of Science and Technology, Aalto University, P.O. Box 11100, FI-00076 Aalto, Finland, NanoMaterials Group, Department of Applied Physics, and Center for New Materials, School of Science and Technology, Aalto University, P.O. Box 15100, FI-00076 Aalto, Finland, and VTT Biotechnology, P.O. Box 1000, FI-02044, Espoo, Finland

Received July 26, 2010; E-mail: maoshuai.he@hut.fi; esko.kauppinen@hut.fi

Abstract: We have developed a magnesia (MgO)-supported iron–copper (FeCu) catalyst to accomplish the growth of single-walled carbon nanotubes (SWNTs) using carbon monoxide (CO) as the carbon source at ambient pressure. The FeCu catalyst system facilitates the growth of small-diameter SWNTs with a narrow diameter distribution. UV–vis–NIR optical absorption spectra and photoluminescence excitation (PLE) mapping were used to evaluate the relative quantities of the different (*n,m*) species. We have also demonstrated that the addition of Cu to the Fe catalyst can also cause a remarkable increase in the yield of SWNTs. Finally, a growth mechanism for the FeCu-catalyzed synthesis of SWNTs has been proposed.

The electrical properties of single-walled carbon nanotubes (SWNTs) depend greatly on their diameter and chirality. To realize most potential applications of SWNTs,¹ one prerequisite is the ability to produce a large quantity of SWNTs exhibiting a single chirality. Different separation techniques have been developed in the past decade to obtain SWNTs as a single (*n,m*) species,^{2,3} though these processes are usually complicated and costly. Therefore, several catalyst systems, such as CoMoCAT⁴ and alcohol CCVD,⁵ have been developed to grow SWNTs with some predominant (*n,m*) species. However, either high pressure in the case of CoMoCAT⁴ or low pressure in the case of alcohol CCVD⁵ has to be applied during the growth process. With methane as a carbon source, an iron–ruthenium (FeRu) catalyst has proven to be efficient for the more desirable growth of (6,5) SWNTs at ambient pressure.⁶ Nevertheless, the use of an expensive noble metal such as Ru might limit the scale-up potential of SWNT production. Furthermore, in all cases, either silica^{4,6} or zeolite,⁵ which is difficult to remove after growth, was selected as catalyst support. It is therefore highly desirable to develop a cheaper catalyst system for selective growth of SWNTs in which the support is easy to remove.

Porous MgO is highly preferred as a catalyst support for SWNT growth because it is easily dissolved by hydrochloric acid (HCl). The MgO used in the experiment was obtained by thermal decomposition of magnesium carbonate hydroxide hydrate. The Fe,

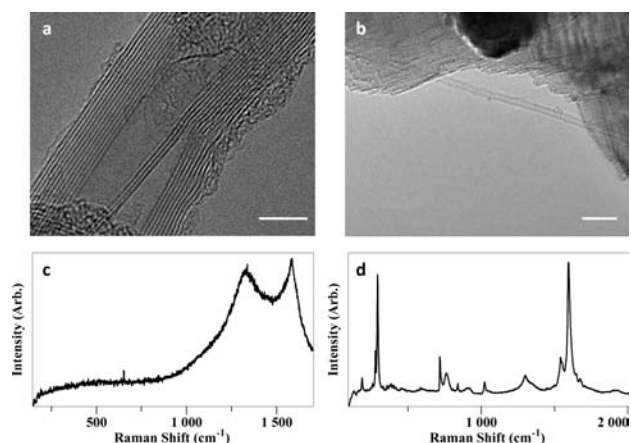


Figure 1. (a, b) TEM images of carbon nanotubes grown on (a) Fe/MgO and (b) FeCu/MgO at 600 °C. Scale bars in both images represent 5 nm. (c, d) Raman spectra (632.8 nm) of (c) carbon nanotubes grown on Fe/MgO at 600 °C and (d) SWNTs grown on FeCu/MgO at 600 °C.

Cu, and FeCu catalysts were deposited on MgO by atomic layer deposition and used for subsequent carbon nanotube growth (Supporting Information I). The Fe catalyst is efficient for dissociating CO and is thus used in, for example, the Fischer–Tropsch synthesis (FTS) because of its good availability and low cost.^{7,8} However, for materials produced using a monometallic Fe/MgO catalyst at 600 °C, only multiwalled carbon nanotubes were observed by transmission electron microscopy (TEM) characterization (Figure 1a and Supporting Information II). This was also verified by the absence of the radial breathing modes (RBMs) in the Raman spectra (Figure 1c). At a higher growth temperature of over 700 °C, SWNTs were observed to grow on the Fe/MgO catalyst, but the yield was relatively low (10% at a growth temperature of 700 °C; Supporting Information III). On the Cu/MgO catalyst, however, no carbon deposition could be achieved under the same growth conditions. This was expected because Cu is a poor catalyst for FTS.⁹ However, it has been demonstrated that SWNTs can grow on Cu catalysts on flat silica substrates.¹⁰

In contrast to the monometallic Fe and Cu catalysts, successful growth of SWNTs on the FeCu catalyst at 600 °C was confirmed by combining TEM characterization (Figure 1b and Supporting Information II) with the Raman spectrum (Figure 1d). The relatively high G/D intensity ratio in the Raman spectrum suggests that the quality of the SWNTs is high. The high-frequency RBMs indicate the presence of small-diameter SWNTs in the product grown at

[†] Department of Biotechnology and Chemical Technology, Aalto University.

[‡] A. M. Prokhorov General Physics Institute.

[§] Department of Applied Physics, Aalto University.

^{||} NanoMaterials Group, Department of Applied Physics, and Center for New Materials, Aalto University.

[⊥] VTT Biotechnology.

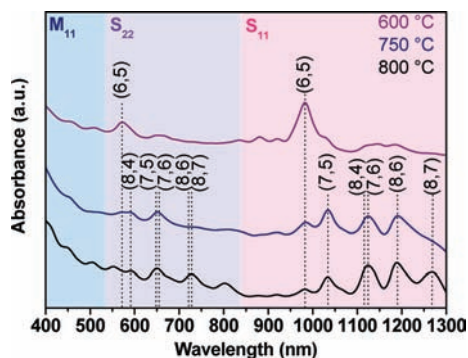


Figure 2. UV-vis-NIR optical absorption spectra of the dispersions of SWNTs grown on FeCu catalysts at temperatures of 600, 750, and 800 °C. S_{11} , S_{22} , and M_{11} represent the wavelength ranges of the lowest-energy semiconducting, second-lowest-energy semiconducting, and lowest-energy metallic absorption peaks, respectively.

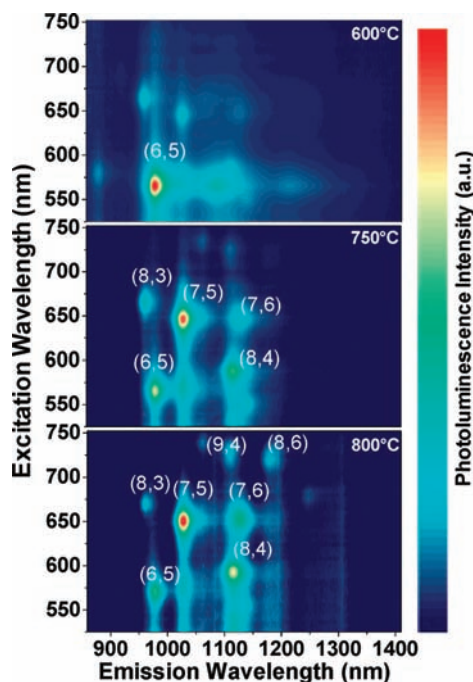


Figure 3. Contour plots of normalized PL emission intensities under various excitation energies for the FeCu SWNTs grown at temperatures of 600, 750, and 800 °C.

600 °C. This observation is in agreement with the data obtained by UV-vis-NIR absorption spectroscopy (Figure 2 and Supporting Information IV) and photoluminescence (PL) spectroscopy (Figure 3, Supporting Information V). Both spectroscopic characterizations were performed on SWNT suspensions that were prepared by sonication of an HCl-purified sample in a sodium cholate hydrate aqueous solution and subsequent centrifugation (more details are presented in Supporting Information IV). In Figure 2, two dominant peaks at 981 and 570 nm, corresponding to the excitation transition energy E_{11} and E_{22} sub-bands for (6,5) tubes, respectively, were observed in the suspension of SWNTs grown at 600 °C. The photoluminescence excitation (PLE) map measurements on the sample also indicated the existence of a majority of (6,5) tubes in the map (Figure 3). The normalized PL emission intensities of different SWNTs species presented in the sample are shown in Figure 4. The PLE (6,5)/(n,m) signal ratios were used to evaluate the relative quantities of the (6,5) tubes.⁶ The (6,5)/(7,5), (6,5)/(8,4), and (6,5)/(7,6) signal intensity ratios were 5, 7, and 13, respectively. All of these values are higher than that obtained for

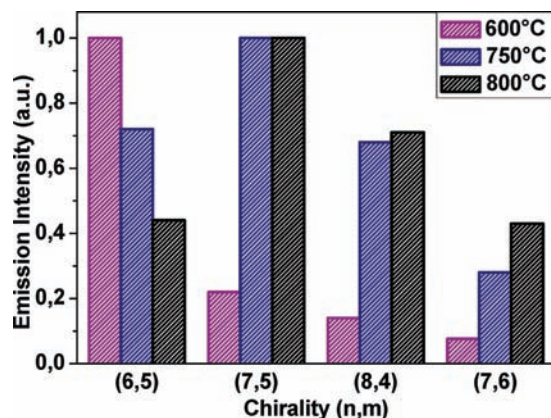


Figure 4. Normalized PL emission intensities of SWNTs grown at temperatures of 600, 750, and 800 °C.

FeRu tubes⁶ or CoMoCAT tube dispersion.⁴ This clearly shows a very high selectivity for (6,5) tubes in the 600 °C growth process.

On the other hand, an increase in the SWNT diameter and a broadening of the diameter distribution at higher growth temperatures were observed, in accordance with previous reports on SWNT synthesis.^{4–6} On the basis of the absorption spectra (Figure 2) and PLE maps (Figure 3) of the samples produced on the FeCu catalyst at 600, 750, and 800 °C, it is easy to discern a trend of increasing SWNT diameter with increasing growth temperature. At a growth temperature of 750 °C, (7,5) tubes became the predominant species; at a growth temperature of 800 °C, (7,5) tubes continued to be the predominant species, but the amounts of (8,4) and (7,6) tubes also increased. Among the samples produced using the FeCu catalyst at different temperatures, the growth temperature of 750 °C provided the most preferable conditions for the growth of (7,5) SWNTs. Moreover, the yields of SWNTs grown at 750 °C on monometallic Fe and FeCu catalysts were compared. It was demonstrated that the FeCu catalyst caused at least a 10-fold increase in the yield of SWNTs (Supporting Information III). This result implies that the presence of Cu in the FeCu catalyst plays a very important role in the SWNT growth process.

To understand the Cu-promoted SWNT growth mechanism, X-ray diffraction (XRD) and X-ray photoelectron spectroscopy (XPS) characterizations of the catalysts were performed. As shown by the XRD patterns of the Fe/MgO, Cu/MgO, and FeCu/MgO catalysts (Supporting Information VI), no indication of alloy formation was found because of the limited miscibility of the two metals in the FeCu/MgO catalyst. The absence of iron oxide reflections in the Fe/MgO and FeCu/MgO patterns suggests that the Fe was well-dispersed in both catalysts. In the XPS spectra (Supporting Information VII), the Fe 2p_{3/2} binding energy in FeCu/MgO was found to be higher than that in Fe/MgO. Meanwhile, a satellite feature¹¹ between the Fe 2p_{3/2} and Fe 2p_{1/2} peaks was observed in the FeCu/MgO spectrum. These observations indicate that more Fe³⁺ is present in the FeCu/MgO catalyst than in Fe/MgO, and this can be interpreted as the result of Fe being deposited adjacent to CuO in the FeCu catalyst.

In comparison with carbon filaments grown on a monometallic Fe catalyst, thinner carbon filaments have been reported to grow on an FeCu catalyst because of the dilution of Fe atoms by Cu in FTS.⁹ It has also been proven that the reduced Cu triggers a reduction of ferric (Fe³⁺) to ferrous (Fe²⁺) ions and a partial reduction to metallic Fe (Fe⁰).^{9,12} In our FeCu catalyst system, the same mechanism is anticipated. Although no H₂ was introduced into the catalyst system, some H₂, which was involved in the water-gas shift reaction, was detected by mass spectrometry during the

growth process (Supporting Information VIII). The reductive CO and H₂, which first reduce CuO to metallic Cu and then adsorb on it, could “spill over” to the adjacent Fe phases and facilitate the reduction of the Fe.¹² Reduced Fe thus forms subnanometer clusters that could be stabilized in the Cu matrix.⁹ Consequently, the SWNT growth that occurs on Fe clusters at Fe–Cu interfaces can be envisaged as the growth of thin carbon filaments.⁹ The reduced metallic Fe clusters are thus supposed to act as the catalyst, leading to the high yield of SWNTs.

In summary, we have developed a FeCu/MgO catalyst that provides a growth predominantly of (6,5) SWNTs at 600 °C. Both the MgO support and the Cu promoter can be removed easily after the growth process. The role of Cu is to enhance the reducibility of Fe and inhibit the aggregation of Fe clusters. As a result, growth of SWNTs is favorable at low temperature, and the yield of SWNTs is greatly enhanced. Both the quality and the purity of the carbon nanotubes are expected to be increased by tuning the ratio between Fe and Cu in the catalyst.

Acknowledgment. This work was supported by TEKES, Academy of Finland (Projects 128445 and 128495), the CNB-E Project in Aalto University through the Multidisciplinary Institute of Digitalization and Energy (MIDE) Program and the RFBR-08-02-91076 Project. We thank Dr. Sanna Airaksinen, Ms. Kati Vilonen, and Ms. Sonja Kouva for useful discussions in the preparation of this manuscript as well as for their experimental support.

Supporting Information Available: Experimental details of the catalyst preparation and the carbon nanotube growth as well as characterizations. This material is available free of charge via the Internet at <http://pubs.acs.org>.

References

- (1) Baughman, R. H.; Zakhidov, A. A.; de Heer, W. A. *Science* **2002**, *297*, 787–792.
- (2) Tu, X. M.; Manohar, S.; Jagota, A.; Zheng, M. *Nature* **2009**, *460*, 250–253.
- (3) Arnold, M. S.; Green, A. A.; Hulvat, J. F.; Stupp, S. I.; Hersam, M. C. *Nat. Nanotechnol.* **2006**, *1*, 60–65.
- (4) Bachilo, S. M.; Balzano, L.; Herrera, J. E.; Pompeo, F.; Resasco, D. E.; Weisman, R. B. *J. Am. Chem. Soc.* **2003**, *125*, 11186–11187.
- (5) Maruyama, S.; Miyachi, Y.; Murakami, Y.; Chiashi, S. *New J. Phys.* **2003**, *5*, 1–12.
- (6) Li, X. L.; Tu, X. M.; Zaric, S.; Welsher, S. K.; Seo, W. S.; Zhao, W.; Dai, H. J. *J. Am. Chem. Soc.* **2007**, *129*, 15770–15771.
- (7) Shroff, M. D.; Kalakkad, D. S.; Coulter, K. E.; Köhler, S. D.; Harrington, M. S.; Jackson, N. B.; Sault, A. G.; Datye, A. K. *J. Catal.* **1995**, *156*, 185–207.
- (8) Krishnankutty, N.; Rodriguez, N. M.; Barker, R. T. K. *J. Catal.* **1996**, *158*, 217–227.
- (9) (a) Weilers, A. F. H.; Koebrugge, G. W.; Geus, J. W. *J. Catal.* **1990**, *121*, 375–385. (b) Weilers, A. F. H.; Hop, C. E. C. A.; van Beujnum, J.; van der Kraan, A. M.; Geus, J. M. *J. Catal.* **1990**, *121*, 364–374.
- (10) Zhou, W. W.; Han, Z. Y.; Wang, J. Y.; Zhang, Y.; Jin, Z.; Sun, X.; Zhang, Y. W.; Yan, C. H.; Li, Y. *Nano Lett* **2006**, *6*, 2987–2990.
- (11) Aronniemi, M.; Sainio, J.; Lahtinen, J. *Surf. Sci.* **2005**, *578*, 108–123.
- (12) de Smit, E.; de Groot, F. M. F.; Blume, R.; Hävecker, M.; Knop-Gericke, A.; Weckhuysen, B. M. *Phys. Chem. Chem. Phys.* **2010**, *12*, 667–680.

JA106609Y